Mismatch Errors in Cascade-Connected Variable Attenuators*

G. E. SCHAFER AND A. Y. RUMFELT†

Summary—**The treatment of mismatch errors is extended to cover variable attenuators cascade-connected in a system which is not free from reflections. The method of analysis is applicable to any number of cascaded attenuators, but only the analysis of two and three variable attenuators in cascade is presented. Graphs are given to aid in estimating the limits of mismatch error.**

In an example, which is considered representative of rigid rectangular waveguide systems, the limits of error are: for two attenuators in cascade, 0.19 db in a 3-db measurement, and 0.17 db in a 40-db measurement; and for three attenuators in cascade, 0.25 db in a 40-db measurement, and 0.23 db in a 75-db measurement.

Introduction

Errors in attenuation caused by the interaction of reflections from generator, attenuator, and load mismatches are termed mismatch errors. Previous treatments of mismatch errors have considered variable or fixed single attenuators in systems with reflections[1,2] and cascaded fixed attenuators in reflection-free systems.[3] In cases where the variable attenuator to be calibrated has a very wide range (greater than 45 db), measurements are often made by using one or two previously calibrated attenuators cascade-connected with the test attenuator (a direct series substitution method). Therefore, the analysis is extended to cascaded variable attenuators in a system which is not free from reflections. Although the method of analysis employed is applicable to any number of variable attenuators in cascade, only the cases of two or three variable attenuators in cascade are presented. Graphs are presented which may be used to estimate the limits of mismatch error in these two cases. An example is given of the use of the graphs. Other sources of error such as the accuracy of the original calibrations, leakage, noise, etc., are not considered here but must be taken into account to obtain total limits of error in an actual calibration.

Theory

In a direct series-substitution method of measuring the attenuation[4] of a variable attenuator, the test attenuator is connected in series with a reference (previously calibrated or standard) attenuator. The total insertion loss of the series-connected pair of attenuators is adjusted to be the same at two different settings. The relative attenuation of the test attenuator is taken to be equal in magnitude to the relative attenuation of the reference attenuator. This is in error because the standard attenuator is connected to a mismatched attenuator, and also because the pair of attenuators are inserted in a mismatched system.

An expression can be derived for the insertion loss of the pair of attenuators connected in cascade. From this, an expression may be written for the difference between the total insertion loss and the sum of the individual attenuations. Inspection of this reveals that the error can be separated into two convenient parts. One of these has been previously worked out[3] in detail for fixed attenuators and is readily extended to variable attenuators, and the other is evaluated here by calculation of certain quantities associated with the combination of attenuators. This separation is performed in the following analysis.

At the initial settings of the attenuators, one may write the total insertion loss as

$$L_i = A_{ti} + A_{ri} + \epsilon_i, \tag{1}$$

where L_i is the total insertion loss at the initial settings of the attenuators, A_{ti} and A_{ri} are the attenuations of the test and reference attenuators at the initial settings, and ϵ_i is the difference between the insertion loss of the pair in cascade and the sum of the individual attenuations. At the final settings of the attenuators, a similar expression for the total insertion loss may be written as

$$L_f = A_{tf} + A_{rf} + \epsilon_f, \tag{2}$$

where the symbols have the same meaning as in (1) except that the subscript f refers to the final settings. The adjustments of the attenuators are made in this way to result in the initial and final total insertion losses being equal, $L_i = L_f$, from which

$$(A_{tf} - A_{ti}) = (A_{ri} - A_{rf}) + \epsilon_T, \tag{3}$$

where ϵ_T has been written for $\epsilon_i - \epsilon_f$. This means that the relative attenuation of the test attenuator may differ from the relative attenuation of the reference attenuator by ϵ_T. This is the desired error. However, a convenient separation may be made as follows. Rewrite (3) as

$$(A_{tf} + A_{rf}) - (A_{ti} + A_{ri}) = \epsilon_T. \tag{4}$$

Let A_i and A_f be the attenuation at the initial and final settings, respectively, of the combination of series-con-

* Manuscript received by the PGMTT, May 4, 1959; revised manuscript received, June 17, 1959.

† U. S. Dept. of Commerce, Natl. Bur. Standards, Boulder Labs., Boulder, Colo.

[1] R. W. Beatty, "Mismatch errors in the measurement of ultrahigh frequency and microwave variable attenuators," *J. Research Natl. Bur. Standards*, vol. 52, pp. 7–9; January, 1954.

[2] C. G. Montgomery, ed., "Technique of Microwave Measurements," Mass. Inst. Tech. Rad. Lab. Ser., McGraw-Hill Book Co., Inc., New York, N. Y., vol. 11, Ch. 13; 1947.

[3] R. W. Beatty, "Cascade-connected attenuators," *J. Research Natl. Bur. Standards*, vol. 45, pp. 231–235; September, 1950.

[4] In this paper, attenuation is defined as the insertion loss in a reflection-free system. Thus, in measuring attenuation, one attempts to eliminate the reflections in the system, and then one measures the insertion loss.

nected attenuators considered as a single attenuator (called the combination attenuator in the remainder of the paper). These may differ from the sums of the individual attenuations by ϵ_{ci} and ϵ_{cf}, respectively, and therefore one may write

$$A_f = A_{tf} + A_{rf} + \epsilon_{cf} \tag{5}$$

$$A_i = A_{ti} + A_{ri} + \epsilon_{ci}. \tag{6}$$

Substituting (5) and (6) into (4) yields

$$A_f - A_i + \epsilon_2 = \epsilon_T, \tag{7}$$

where ϵ_2 has been written for $\epsilon_{ci}-\epsilon_{cf}$. The component ϵ_2 of the mismatch error is the difference between the attenuation of the combination attenuator and the sums of the attenuations of the individual attenuators. This component may be evaluated by an extension of the results of Ref. 3 to include the case of variable attenuators connected in cascade, and may be written as

$$\epsilon_2 = 20 \log_{10} \left| \frac{1 - {}^{(f)}S_{11}'' {}^{(f)}S_{22}'}{1 - {}^{(i)}S_{11}'' {}^{(i)}S_{22}'} \right|, \tag{8}$$

where the front superscripts (i) and (f) refer to the initial and final values, respectively; the primed S's are elements of the scattering matrices[5] of the individual attenuators, and the number of primes indicate the position of the attenuator as counted from the generator.

Eq. (7) may be written as

$$A_f - A_i = \epsilon_T - \epsilon_2 = \epsilon_1. \tag{9}$$

This form is equivalent to considering the combination attenuator as a single attenuator at two different attenuation settings, and ϵ_1 can therefore be evaluated as the mismatch error in a relative attenuation measurement with a single attenuator. This component of mismatch error has been treated by Beatty[1] and for this application may be written as

$$\epsilon_1 = 20 \log_{10} \left| \frac{(1 - {}^{(f)}\Gamma_1\Gamma_9)(1 - {}^{(f)}S_{22}\Gamma_L)}{(1 - {}^{(i)}\Gamma_1\Gamma_9)(1 - {}^{(i)}S_{22}\Gamma_L)} \right|, \tag{10}$$

where the front superscripts (i) and (f) refer to the initial and final values, respectively, and where Γ_1 is the input reflection coefficient of the combination attenuator when terminated with an equivalent detector having a reflection coefficient Γ_L. Also, Γ_G is the reflection coefficient of the equivalent generator, and S_{22} is an element of the scattering matrix, S, of the combination attenuator. It should be recalled that this expression gives smaller limits of mismatch error than the addition of the separate limits of mismatch error for attenuation at the initial and final settings.

The total error in cascading variable[6] attenuators in a mismatched system is then $\epsilon_1+\epsilon_2$, where ϵ_1 is the error caused by interactions of reflections from the generator, combination attenuator, and the load, and ϵ_2 is the error caused by interactions of reflections from the individual attenuators.

The scattering matrix of the combination attenuator is used to evaluate the component ϵ_1 of the mismatch error according to (10). This is readily obtained in terms of the scattering matrices of the individual attenuators through use of the T matrices.[7] The T matrix for a combination of n cascade-connected attenuators may be written as

$$T = \prod_{k=n}^{k=1} T_k, \tag{11}$$

where the T_k are the matrices for the individual attenuators. This T matrix is the inverse of the A matrix used in Ref. 3. The scattering matrix, S, for the two-arm junction is related to the T matrix as follows:

$$S = \frac{1}{T_{22}} \begin{vmatrix} -T_{21} & 1 \\ 1 & T_{12} \end{vmatrix} \text{ and } T = \frac{1}{S_{12}} \begin{vmatrix} S_{12}^2 - S_{22}S_{11} & S_{22} \\ -S_{11} & 1 \end{vmatrix}, \tag{12}$$

when reciprocity in the form $S_{pq}=S_{qp}$ is assumed. The necessary characteristics of the combination of attenuators needed to evaluate the error by (10) are Γ_1 and S_{22}. These may be obtained by use of (11) and (12), and the expression

$$\Gamma_1 = S_{11} + \frac{S_{12}^2\Gamma_L}{1 - S_{22}\Gamma_L}. \tag{13}$$

The results for two attenuators in cascade are

$$\Gamma_1 = S_{11}' + \frac{(S_{12}')^2 S_{11}''(1 - S_{22}''\Gamma_L) + (S_{12}')^2(S_{12}'')^2\Gamma_L}{(1 - S_{22}''\Gamma_L)(1 - S_{11}''S_{22}') - S_{22}'(S_{12}'')^2\Gamma_L}, \tag{14}$$

and

$$S_{22} = S_{22}'' + \frac{S_{22}'(S_{12}'')^2}{1 - S_{11}''S_{22}'}, \tag{15}$$

and for three attenuators in cascade, they are

$$\Gamma_1 = S_{11}' + \frac{(S_{12}')^2\{S_{11}''[(1 - S_{22}''S_{11}''')(1 - S_{22}'''\Gamma_L) - S_{22}''(S_{12}''')^2\Gamma_L] + S_{11}'''(S_{12}'')^2(1 - S_{22}'''\Gamma_L) + (S_{12}'')^2(S_{12}''')^2\Gamma_L\}}{(1 - S_{22}'''\Gamma_L)[(1 - S_{22}'S_{11}'')(1 - S_{22}''S_{11}''') - S_{22}'(S_{12}'')^2S_{11}'''] - (S_{12}''')^2\Gamma_L[S_{22}''(1 - S_{11}''S_{22}') + S_{22}'(S_{12}'')^2]}, \tag{16}$$

and

$$S_{22} = S_{22}''' + \frac{(S_{12}''')^2\{S_{22}'(S_{12}'')^2 + S_{22}''(1 - S_{11}''S_{22}')\}}{(1 - S_{22}'S_{11}'')(1 - S_{11}'''S_{22}'') - S_{22}'S_{11}'''(S_{12}'')^2}, \tag{17}$$

[5] C. G. Montgomery, *op. cit.*, Ch. 14.

[6] The same analysis applies to cascaded-fixed, or a combination of fixed and variable attenuators in a mismatched system by using the appropriate forms of (8) and (10).

[7] C. G. Montgomery, R. H. Dicke, and E. M. Purcell, "Principles of Microwave Circuits," Mass. Inst. Tech. Rad. Lab. Ser., McGraw-Hill Book Co., Inc., New York, N. Y., vol. 8, Ch. 5; 1948.

where the primed S's are the scattering coefficients of the individual attenuators, where the number of primes indicates the position of the attenuator as counted from the generator end where Γ_L is the equivalent reflection coefficient of the detector, and where reciprocity in the form $S_{pq}=S_{qp}$ has been assumed.

Substitution of (14) and (15) into (10) gives the expression for the component ϵ_1 of the mismatch error for two variable attenuators in cascade. Similarly, substitution of (16) and (17) gives the corresponding expression for the case of three variable attenuators in cascade.

Assuming that the phases of the individual coefficients of (8) and (10) are not known and that they can have any possible value, the actual values of the error components cannot be determined, but limits may be found. Such a limit is a conservative figure, and a closer estimate of the actual error may be obtained if one determines the phases of the individual coefficients. The limits of ϵ_1 and ϵ_2 may be added to obtain limits of the mismatch error, ϵ_T, since the phases of the coefficients in (8) and (10) can take on values so that each component of mismatch error is simultaneously at its maximum possible value.

Graphical Presentation of Results

One of the factors taken into consideration, in constructing the graphs, was the ease of obtaining an estimate of the limits of the mismatch error. For this purpose, certain assumptions to be discussed were made concerning the scattering coefficients of the attenuators. Since many commercially available attenuators have similar voltage-standing-wave ratio (VSWR) characteristics, it will become evident that these assumptions caused very little loss in the generality of application. The following equalities were assumed:

$$\begin{aligned} |S_{11}'| &= |S_{11}''| = |S_{11}'''| = |S_{22}'| \\ &= |S_{22}''| = |S_{22}''| \end{aligned} \tag{18}$$

and

$$|\Gamma_G| = |\Gamma_L|. \tag{19}$$

Furthermore, it was assumed that the phases of each coefficient in (14)–(17) and the S_{12}'s took on values at the initial and final settings of the attenuators which would give the maximum possible mismatch error (limits of mismatch error). This assumption yields a conservative estimate of the mismatch error.

The range of the limits of the mismatch error, ϵ_T, for two attenuators in cascade and for three attenuators in cascade are shown in Figs. 1 and 2, respectively. The sectors indicate how the limits of error vary with the number of decibels to be measured and with the VSWR of the attenuators for a number of specified equivalent generator and detector mismatches. Eq. (18) implies

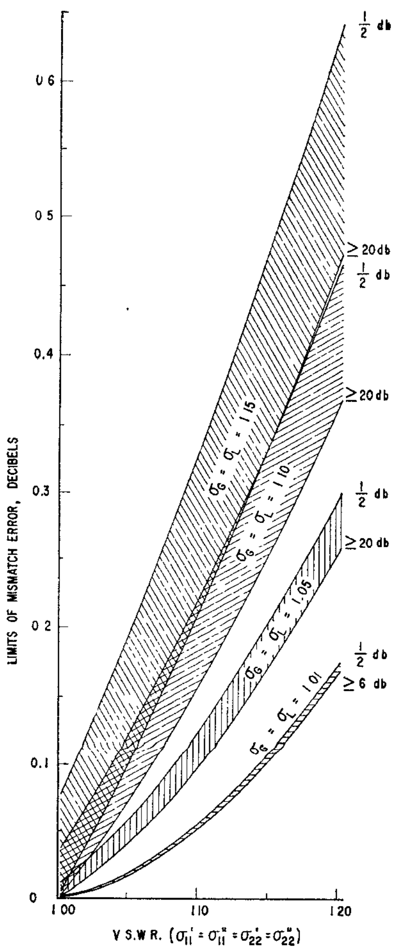

Fig. 1—Variation with range of measurement in limits of mismatch error, ϵ_T, for two variable attenuators in cascade.

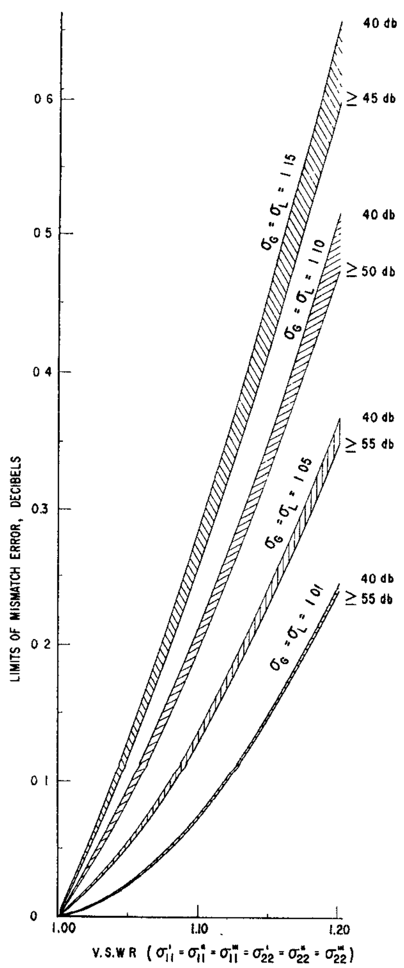

Fig. 2—Variation with range of measurement in limits of mismatch error, ϵ_T, for three variable attenuators in cascade.

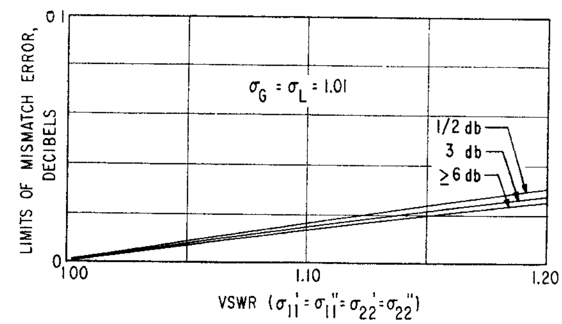

Fig. 3—Limits of component ϵ_1 of mismatch error for two attenuators with equal magnitudes of S_{11} and S_{22} cascaded in a system where $\sigma_G = \sigma_L = 1.01$.

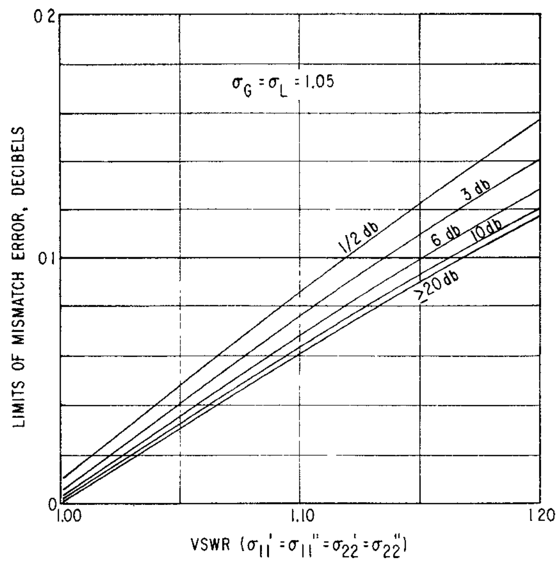

Fig. 4—Limits of component ϵ_1 of mismatch error for two attenuators with equal magnitudes of S_{11} and S_{22} cascaded in a system where $\sigma_G = \sigma_L = 1.05$.

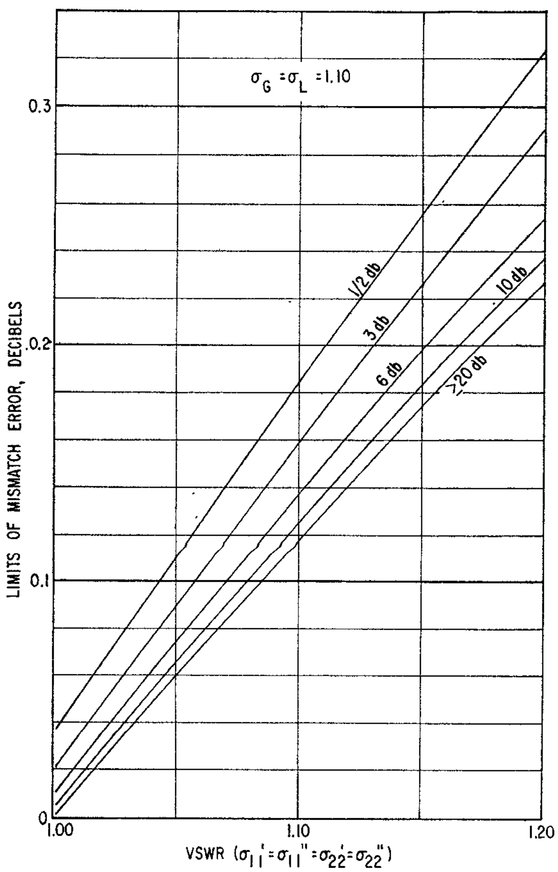

Fig. 5—Limits of component ϵ_1 of mismatch error for two attenuators with equal magnitudes of S_{11} and S_{22} cascaded in a system where $\sigma_G = \sigma_L = 1.10$.

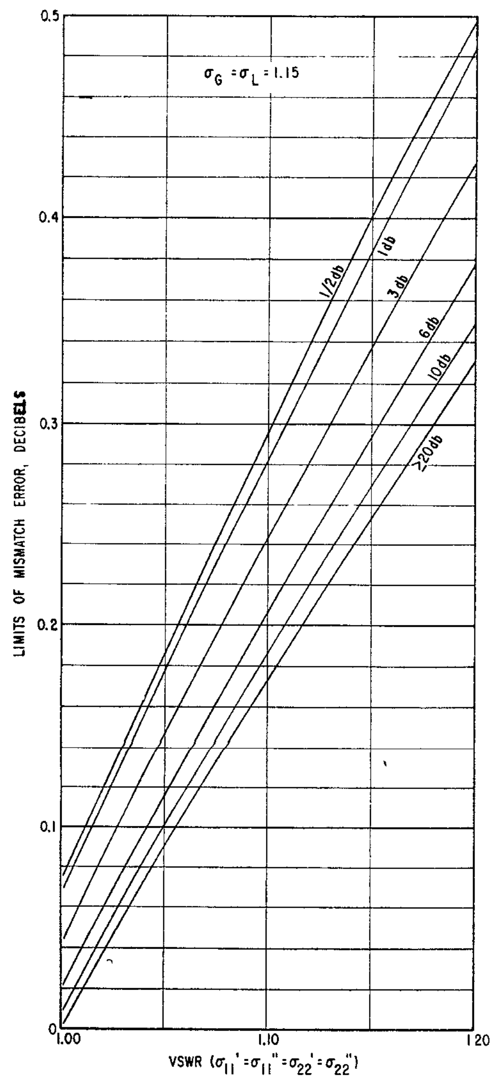

Fig. 6—Limits of component ϵ_1 of mismatch error for two attenuators with equal magnitudes of S_{11} and S_{22} cascaded in a system where $\sigma_G = \sigma_L = 1.15$.

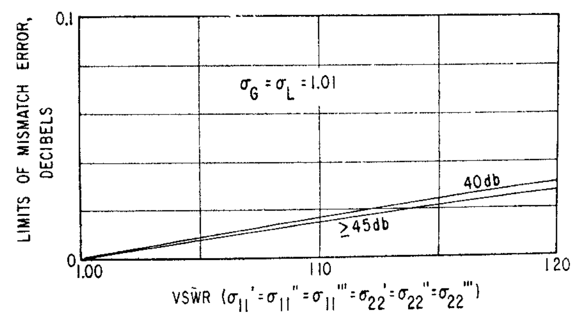

Fig. 7—Limits of component ϵ_1 of mismatch error for three attenuators with equal magnitudes of S_{11} and S_{22} cascaded in a system where $\sigma_G = \sigma_L = 1.01$.

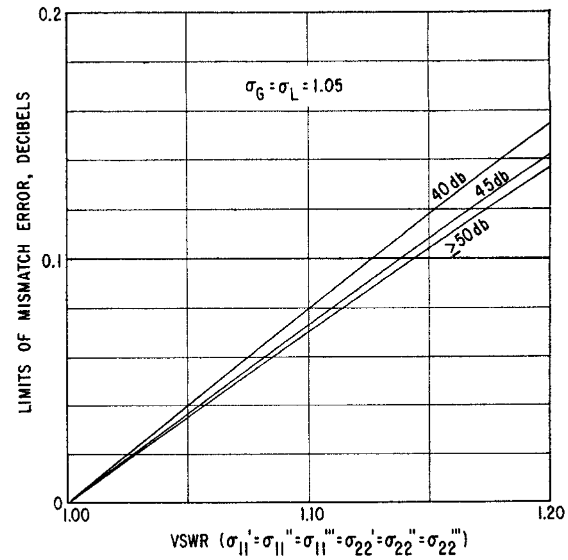

Fig. 8—Limits of component ϵ_1 of mismatch error for three attenuators with equal magnitudes of S_{11} and S_{22} cascaded in a system where $\sigma_G = \sigma_L = 1.05$.

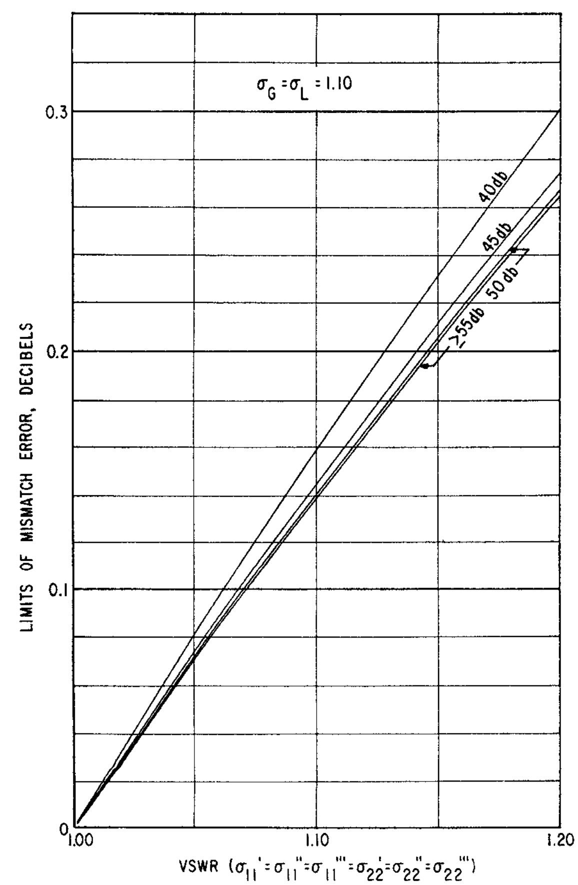

Fig. 9—Limits of component ϵ_1 of mismatch error for three attenuators with equal magnitudes of S_{11} and S_{22} cascaded in a system where $\sigma_G = \sigma_L = 1.10$.

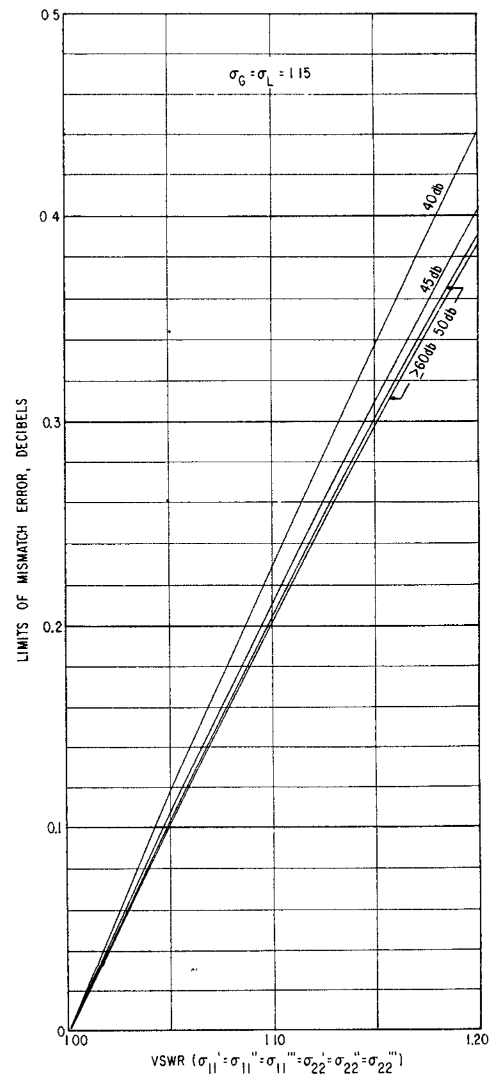

Fig. 10—Limits of component ϵ_1 of mismatch error for three attenuators with equal magnitudes of S_{11} and S_{22} cascaded in a system where $\sigma_G = \sigma_L = 1.15$.

that the VSWR corresponding to S_{11} or S_{22} of the attenuators, which is the abscissa, has been assumed to be the same and equal for the input and output of each attenuator. Each sector is labeled with the appropriate values of the VSWR associated with the equivalent generator and detector reflection coefficients which were assumed to be equal in (19). The ordinates are the limits of mismatch error. These figures are presented to illustrate the range of limits of mismatch error to be expected in the assumed situations.

Figs. 3–6 are a series of graphs of the limits of the component ϵ_1 of mismatch error for two attenuators in cascade with σ_G $(=\sigma_L)$ of 1.01, 1.05, 1.10, and 1.15, respectively. σ_G and σ_L are the VSWR's associated with the equivalent generator and detector reflection coefficients, respectively. The VSWR's used as the abscissas are the input and output VSWR's of the variable attenuators. It is assumed that these VSWR's are all equal. The parameter for the family of curves is the number of decibels to be measured by this technique.

Figs. 7–10 are an equivalent series of graphs of the limits of the component ϵ_1 of the mismatch error for the case of three attenuators in cascade. These are applicable for measurements of attenuation of 40 db or more.

Figs. 11 and 12 are graphs of the limits of the component ϵ_2 of the mismatch error for the cases of two and three attenuators in cascade. The abscissas are the VSWR's of the attenuators. The limits of error in this case are independent of the load and generator mismatches. For the case of three attenuators in cascade, Fig. 12 is constructed on the assumption that at least 20 db attenuation is in the middle attenuator at one of the attenuation settings, either the initial or the final.

Use of the Graphs

In order to use the graphs of Figs. 3–12 to estimate the limit of error, one must know the VSWR's of the attenuators and of the equivalent generator and detector, and the approximate number of decibels to be measured. For an example, consider a case where 1) the equivalent generator and detector VSWR's are 1.03 and 1.04, respectively; 2) the three attenuators have input and output VSWR's of 1.15 or less; and 3) the desired attenuation measurements are 3 db, 40 db, and 75 db, and the reference attenuators are calibrated up to 40 db. The values of the generator and detector VSWR's are used to determine which of the graphs of ϵ_1 is to be used. One selects the graph with the nearest available value of $\sigma_G(=\sigma_L)$ which is equal to, or greater than, the larger value of the actual load or generator VSWR. This will give a conservative estimate of the limits of error. In this example, the actual VSWR's of the generator and the detector are 1.03 and 1.04, respectively, and for the case of two attenuators in cascade, Fig. 4 would be selected, since it is constructed on the assumption that both of these are 1.05. Having selected the graph, the largest value of the VSWR at the input or output of the attenuators is the abscissa. Typical commercially-available attenuators for rectangular waveguide systems have maximum VSWR of 1.15 over their entire frequency and attenuation ranges. For a conservative estimate, then, one could use an abscissa of 1.15 unless the actual values of the VSWR are known to be different. The value of ϵ_1 is different for different values of attenuation. For a 3-db measurement it has the value 0.11 db, and for a 40-db measurement it is 0.09 db. Note that for measurements of attenuation of 20 db or greater the component ϵ_1 of the limits of error does not change within the resolution of the graphs.

One determines ϵ_2 from Fig. 11, and it depends only on the VSWR's of the attenuators, and not on the amount of attenuation or on the generator and load mismatches. For a VSWR of 1.15, ϵ_2 is 0.08 db. Addition of these two components, as determined from Figs. 4 and 11, yields the limits of mismatch error, ϵ_T, of 0.19

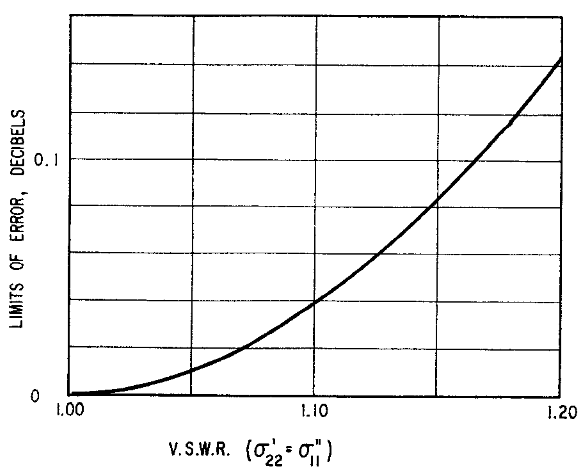

Fig. 11—Limits of component ϵ_2 of mismatch error for two attenuators with equal magnitudes of S_{11} and S_{22}.

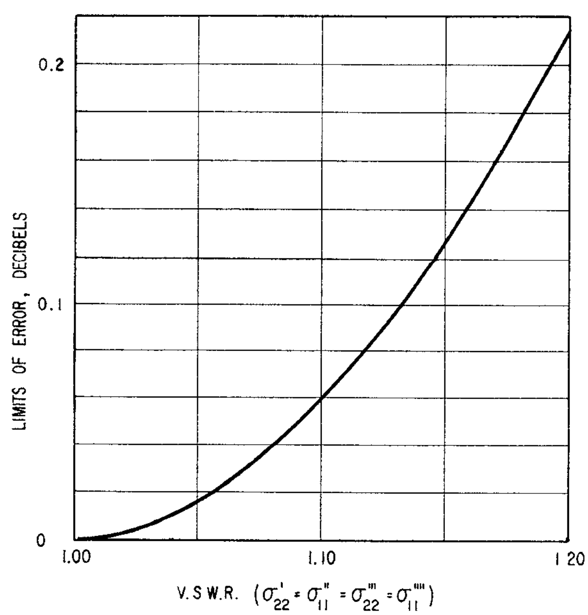

Fig. 12—Limits of component ϵ_2 of mismatch error for three attenuators with equal magnitudes of S_{11} and S_{22}.

db for a 3-db measurement and 0.17 db for a 40-db measurement.

If the three similar attenuators are connected in cascade and inserted in the system, Fig. 8 shows that ϵ_1 is now 0.12 db for a 40-db measurement and 0.10 db for a 75-db measurement, and Fig. 12 shows that ϵ_2 is 0.13 db for both measurements. Addition of these yields the limits of mismatch error, ϵ_T, of 0.25 db for a 40-db measurement and 0.23 db for a 75-db measurement. These examples are felt to be representative of conditions met in typical rectangular waveguide systems.

Conclusion

It can be seen that if maximum possible error is assumed, the mismatch error increases for smaller relative attenuation measurements.

The limit of mismatch error estimated by this method is a conservative figure since it is based on the assumption that all values of the coefficients have phases at the initial and final settings which give the maximum possible error. Thus, in an actual application, the mismatch errors are very probably less than those estimated in the examples.

A Nonreciprocal, TEM-Mode Structure for Wide-Band Gyrator and Isolator Applications*

E. M. T. JONES†, G. L. MATTHAEI†, AND S. B. COHN†

Summary—**The theoretical and experimental operation of a novel form of TEM transmission-line network capable of operation over octave bandwidths is described. This network consists, basically, of a parallel arrangement of two conductors and a ferrite rod within a grounded outer shield. The conductors may be connected in a two-port configuration which provides, in the absence of the ferrite rod, complete isolation from zero frequency to the cut-off frequency of the first higher mode. With an unmagnetized ferrite rod properly inserted, the broad-band isolation is virtually unaffected. When the rod is magnetized by an axial magnetic field, coupling occurs between the two ports by a process analogous to Faraday rotation.**

The device may be used as a broad-band gyrator, switch, or modulator, and with the addition of a resistance load, as an isolator. The bandwidth of these components is inherently limited only by the bandwidth capability of the ferrite material itself.

I. Qualitative Description of Operation

Gyrator Network

THE form of the nonreciprocal TEM transmission-linenet work that functions as a wide-band gyrator, switch, or modulator is illustrated in Fig. 1.[1-3] It consists of a pair of shielded, coupled transmission lines and an axially oriented ferrite pencil. This circuit behaves, in the absence of the ferrite rod, as an all-stop filter; *i.e.*, infinite attenuation theoretically exists between the two ports at all frequencies.[4] For the network to be an all-stop filter, it is necessary that one of the coupled lines be open-circuited and the other short-circuited, in the manner shown in the figure, and that the phase velocity of the even and odd modes on the coupled lines be the same. Both these conditions are satisfied when the ferrite is properly oriented in the plane of symmetry between the coupled lines. The proper position of the rod is quite independent of frequency, so that the composite structure has high attenuation over a wide band of frequencies.

When an axial magnetic field is applied to the ferrite rod, it rotates the plane of polarization of the linearly polarized transverse RF magnetic field existing along the ferrite rod, and energy is coupled between the input and output ports. When the axial field is increased to the point where the RF magnetic field is rotated by 90 degrees, virtually all the energy is transferred. When the cross section of the ferrite rod is small in terms of wavelength, and the operating frequency is far removed from the ferromagnetic resonance frequency, the rotation of the plane of polarization per unit length by the ferrite is essentially independent of frequency. Therefore, low insertion loss is experienced over a wide frequency range. Because the plane of polarization of the RF magnetic field is rotated in the same sense with respect to the positive direction of the biasing magnetic field, independent of the direction of propagation through the

* Manuscript received by the PGMTT, April 29, 1959; revised manuscript received, June 19, 1959.

† Div. of Engrg. Res., Stanford Res. Inst., Menlo Park, Calif.

[1] E. M. T. Jones, S. B. Cohn, and J. K. Shimizu, "A wide-band nonreciprocal TEM-transmission-line network," 1958 WESCON Convention Record, pt. 1, pp. 131–135.

[2] O. W. Fix, "A balanced-stripline isolator," IRE Convention Record, pp. 99–105; March, 1956.

[3] H. Boyet and H. Seidel, "Analysis of nonreciprocal effects in an N-wire ferrite-loaded transmission line," Proc. IRE, vol. 45, pp. 491–495; April, 1957.

[4] E. M. T. Jones and J. T. Bolljahn, "Coupled-strip-transmission-line filters and directional couplers," IRE Trans. on Microwave Theory and Techniques, vol. MTT-4, pp. 75–81; April, 1956.